Soil Dynamics and Earthquake Engineering 25 (2005) 461–469
SOIL DYNAMICS AND EARTHQUAKE ENGINEERING
www.elsevier.com/locate/soildyn

Correlation of shear wave velocity with liquefaction resistance based on laboratory tests

Chen Yunmin*, Ke Han, Chen Ren-peng

Civil Engineering Department, Institute of Geotechnical Engineering, Zhejiang University, Hangzhou 310027, People's Republic of China

Accepted 18 March 2005

Abstract

According to the results of cyclic triaxial tests on Hangzhou sands, a correlation is presented between liquefaction resistance and elastic shear modulus. Material-dependent but independent of confining stress, shows the linear relation of $(\sigma_d/2)^{1/2}$ with G_{max}. For its application to different soils, a method proposed by Tokimatsu [Tokimatsu K, Uchida A. Correlation between liquefaction resistance and shear wave velocity. Soils Found 1990:30(2):33–42] is utilized to normalize the shear modulus with respect to minimum void ratio. A simplified equation is established to evaluate the liquefaction potential by shear-wave velocity. The critical shear-wave velocity of liquefaction is in linear relation with 1/4 power of depth and the peak horizontal ground surface acceleration during earthquakes. The equation proposed in this paper is compared with previous methods especially the procedure proposed by Andrus [RD Andrus, KH Stokoe. Liquefaction resistance of soils from shear-wave velocity. J Geotech Geoenviron Eng 2000:126(11):1015–25]. The results show its simplicity and effectiveness when applied to sands, but more validation or modification is needed for its application to sand with higher fines content.

Keywords: Liquefaction; Shear wave velocities; Dynamic triaxial test; Minimum void ratio

1. Introduction

Recently, the shear wave velocity of soils is used in earthquake engineering and geotechnical engineering on an increasing scale. In the field of evaluation of soils' liquefaction resistance, it has also been drawn more attention as a promising alternative, or supplement, to the penetration-based approaches according to its advantages [1]. Some in-situ tests show that the values of shear wave velocity measured by cross-hole tests, downhole tests, SCPT tests and SASW tests agree well with each other in the depth of 5–8 m [2]. As a whole, the precision of different kinds of shear-wave velocity tests is higher than that of SPT tests. The feasibility of the evaluation is mainly due to the physical foundation that many factors such as relative density, soil fabric, prior earthquake strains affect the liquefaction resistance and shear wave velocity in the same direction [3,8].

Dobry [13] discovered the existence in sands of a threshold shear strain γ_t, of the order of 10^{-2}%, which makes it feasible to evaluate soil's liquefaction susceptibility by shear wave velocity. Over the 20 years since then, numerous studies have been conducted to get the correlation between shear wave velocity and liquefaction potential of soils or sands. And there are several ways to establish this correlation [1,3]:

(1) Methods based on a combination of in situ measurements of shear wave velocity and laboratory liquefaction tests [3,4]. The concept of the method lies in the fact that the same type of soils, which have the same shear wave velocity under the same stress conditions, may have the same liquefaction resistance.
(2) Methods based on in-situ measurements of shear wave velocity and an appropriate correlation between liquefaction resistance and shear wave velocity. Some field correlations [1,5] have been presented to support the feasibility of this approach.
(3) Other methods including penetration—V_s correlation [6,7].

* Corresponding author.
E-mail addresses: cym@civil.zju.edu.cn (C. Yunmin), kehanzj@sina.com.cn (K. Han), crp@civil.zju.edu.cn (C. Ren-peng).

0267-7261/$ - see front matter © 2005 Elsevier Ltd. All rights reserved.
doi:10.1016/j.soildyn.2005.03.003

Because of its repeatability and maneuverability, the first procedure above is preferred in this paper. However, the field performance data collected and summarized in the workshop paper by Stokoe [1] are utilized to make the proposed correlation more agreeable to the field performance.

2. Surmised correlation between liquefaction resistance and shear modulus

By means of cyclic triaxial tests on six kinds of sands, De Alba [4] suggested that there exists a satisfying correlation between elastic-wave velocity and liquefaction resistance under the identical confining stress. This conclusion implies that the field measurements of elastic-wave velocities may be used to reconstitute laboratory specimens to their in-place liquefaction resistance [8]. Tokimastu [8] showed that a reasonable correlation would exist between liquefaction characteristics and elastic shear modulus for a given soil under given confining stresses. Based on this conclusion, Tokimastu and Uchida [3] proposed a method of estimating the liquefaction potential by shear wave velocity and obtained a satisfactory result. These studies provided the experimental base to get theoretical correlation between liquefaction potential and elastic shear modulus.

It is widely acknowledged that the liquefaction resistance of a kind of soil is proportional to the effective stress [3,9]:

$$\tau_d = \frac{\sigma_d}{2} \propto \sigma'_m \tag{1}$$

in which $\sigma'_m = (1 + 2K_0/3)\sigma'_v$, is the vertical effective confining pressure, and K_0 is the earth pressure coefficient at rest.

In general, elastic shear modulus G_{max} is given as follows (e.g. Hardin and Richart, 1963)

$$G_{max} = AF(e)(\sigma'_m)^n \tag{2}$$

n is a constant approximately equal to 0.5 and A is a constant reflecting soil fabric, etc. so:

$$G_{max} \propto (\sigma'_m)^{1/2} \tag{3}$$

Tokimatsu [8] has demonstrated that the same type of soils, which have the same shear wave velocity under the same confining pressure may have the same liquefaction resistance. So if it is validated further that the change of confining pressure will influence the increment or decrement of shear wave velocity and liquefaction resistance in the same way as other factors (e.g. relative density, small seismic strain history and consolidation history), there may exist good correlation between $(\sigma_d/2)$ and G_{max}. And the correlation could be defined from Eqs. (1) and (3) as follows:

$$\tau_d = \frac{\sigma_d}{2} \propto G_{max}^2 \tag{4}$$

3. Laboratory tests and results

Tests are designed to investigate the contribution of stress conditions as well as other factors to the increment of shear wave velocity and liquefaction resistance. Two series of dynamic triaxial tests were devised to obtain these goals: (1) control the shear wave velocity by changing the relative density or strain history with the confining stress (100 kPa) unchanged. (2) Control the shear wave velocity by changing its confining pressure with the relative density (60%) unchanged.

Bender element was installed on the conventional dynamical triaxial tests system so that both measurements of shear wave velocity and dynamical triaxial tests could be conducted consecutively on the same samples [14,15]. The generation and receiving of the shear wave are carried out by the Bender Element, which was also used to determine the shear-wave velocity. The bender was first used to determine the V_s of soil's specimen by De Alba [4]. The sands used in these tests are obtained from two sites: Hangzhou and Fujian. The physical properties are listed in Table 1.

To obtain different soil fabrics, the sand samples approximately 125 mm high and 50 mm in diameter were prepared by different techniques described by Tomimatsu [8]. The test specimens include those obtained by pluviation through air (PA samples), and those subjected to small seismic strain history (SH samples) and over-consolidation history (OC samples).

In the first series of tests, the confining pressure is fixed as 100 kPa and the range of the relative density is from 40 to 80%. De Alba [4] assumed that the liquefaction potential of a site is most debatable within the range 50–80%.

τ_{15} is defined as the liquefaction resistance ($\sigma_d/2$) to cause a double amplitude axial strain of 5% in 15 cycles in this paper. The liquefaction defined in terms of strain is adopted because the 100% pore pressure of some samples is means to unacceptable deformation. Admittedly, the strain criterion may or may not imply 100% pore pressure. Since the field decision on whether the site liquefied or not is usually based on surface phenomena and is often associated with 100% pore pressure, so this definition probably affects the comparison of lab and field correlations to some extent.

As a reference, τ_0 is defined as τ_{15} of PA samples when the relative density is 60% and the confining pressure is 100 kPa and due G_{max} is defined as G_0. τ_{15}/τ_0 is plotted in Fig. 1 against G_{max}/G_0 with different relative density

Table 1
Physical properties of Hangzhou sand

Location	G_s	D_{10}	U_c	F_c (%)	e_{min}	e_{max}
Hangzhou	2.69	0.12	2.4	1.0	0.55	1.25
Fujian	2.71	0.13	3.0	0.0	0.43	0.79
Niigata	2.69	0.18	1.8	0.4	0.77	1.23
Toyoura	2.64	0.16	1.4	0.0	0.61	0.99

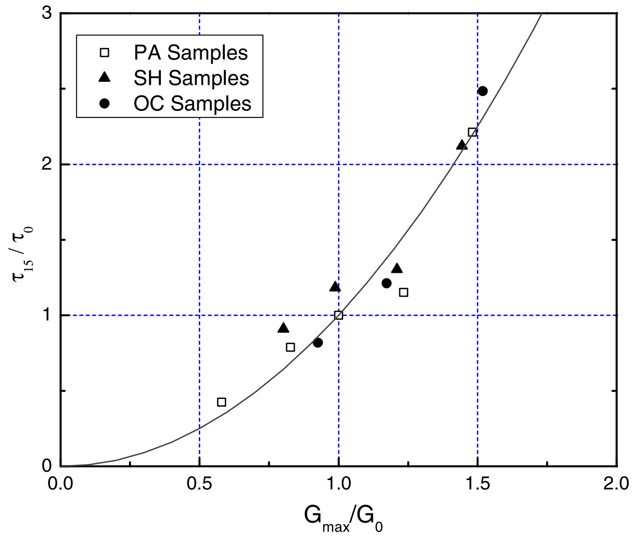

Fig. 1. Relationship between G_{max}/G_0 and τ_{15}/τ_0 for PA, SH and OC samples from Hangzhou under the same confining stress (100 KPa).

and the same confining stress (100 kPa). For the convenience of comparison, the shear modulus of SH samples are controlled to have almost the same shear modulus of one PA Sample. It can be seen that the liquefaction characteristics could be reasonably well correlated with shear modulus for a given soil under the same confining pressure, no matter whether it is PA samples, SH samples or OC samples.

In the second series of cyclic triaxial tests, the PA samples have the same relative density (60%) under different confining pressures. To simulate field k_0 conditions, two values of k_0 were adopted in the second series of cyclic triaxial test: 1.0 and 0.5. The result of τ_{15}/τ_0 is plotted in Fig. 2 against G_{max}/G_0.

Figs. 1 and 2 display the similarities between the two best-fit curves of the data. For the clearer demonstration,

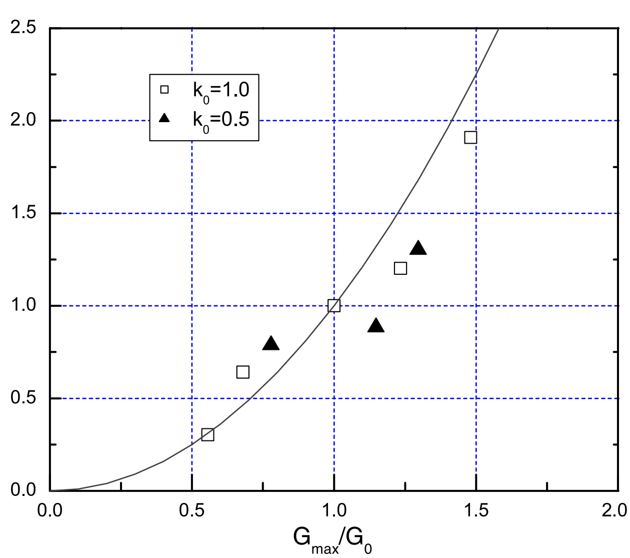

Fig. 2. Relationship between G_{max}/G_0 and τ_{15}/τ_0 for PA samples with the same relative density.

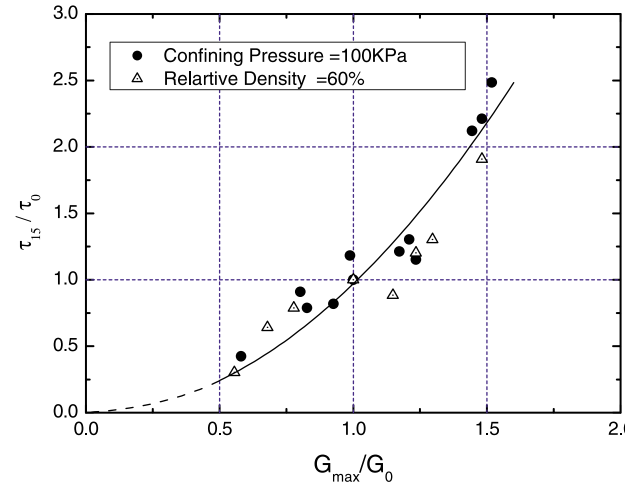

Fig. 3. Relationship between G_{max}/G_0 and τ_{15}/τ_0 for Hangzhou Sand.

the data of these two series results are plotted in Fig. 3. It is shown different factors such as relative density, confining stress, soil fabric, K_0, prior strain history and over-consolidation influence the liquefaction resistance ($\sigma_d/2$) and shear modulus almost in the same way. In another word, for the same soil, a approximate correlation exist between liquefaction resistance ($\sigma_d/2$) and shear modulus, regardless of its confining stress.

To validate Eq. (4), the results of Hangzhou and Fujian soils are plotted in Fig. 4 with the horizontal coordinate G_{max}/G_0 and the vertical coordinate $(\tau_{15}/\tau_0)^{1/2}$. Because there is not sufficient data, the results of Niagata soils done by Tokimatsu et al. [3,8] are plotted in Fig. 5 with the horizontal coordinate G_{max} and the vertical coordinate $(\tau_{15})^{0.5}$ (KPa)$^{0.5}$. From Figs. 4 and 5, it can be seen that for the same soil, all data are limited to a narrow band and are well fitted by a line projected back through the origin.

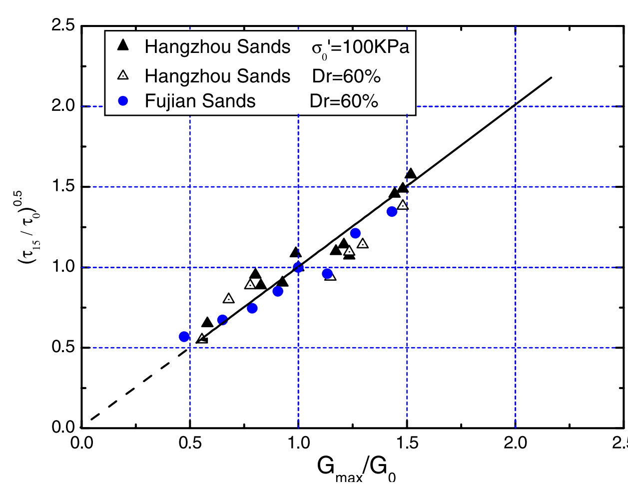

Fig. 4. Relationship between G_{max}/G_0 and $(\tau_{15}/\tau_0)^{0.5}$ for Hangzhou and Fujian sands.

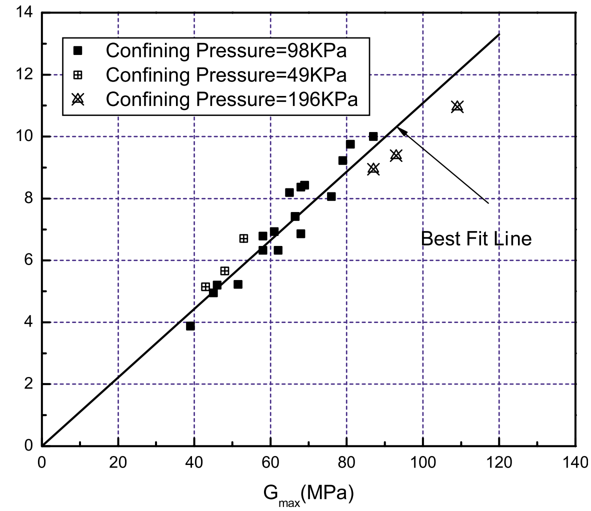

Fig. 5. Relationship between G_{max}/G_0 and $(\tau_{15}/\tau_0)^{0.5}$ for Niagata sands.

To compare different correlation of the soils come from different places, the results of Hangzhou soils, Fujian soils, Niigata soils, and Toyoura soils [3] are plotted in Fig. 6, and the physical properties are listed in Table 1.

Fig. 6 shows a poor correlation between τ_{15} and G_{max} and similar results will be obtained if the vertical coordinate is supplemented by τ_{15}/σ'_m. In order to correct for the effects of difference in soil type, a method proposed by Tokimatsu and Uchida [3] was adopted. The horizontal coordinate G_{max} was normalized by $F(e_{min})$, where $F(e)$ is the function proposed by Hardin (1963) $(2.17-e)^2/1+e$. Fig. 7 shows the effectiveness of the normalization with the vertical coordinate $(\tau_{15})^{1/2}$, with all data falling close to a line projected back through the origin. Though the Toyoura sands are slightly more scattered than the other two.

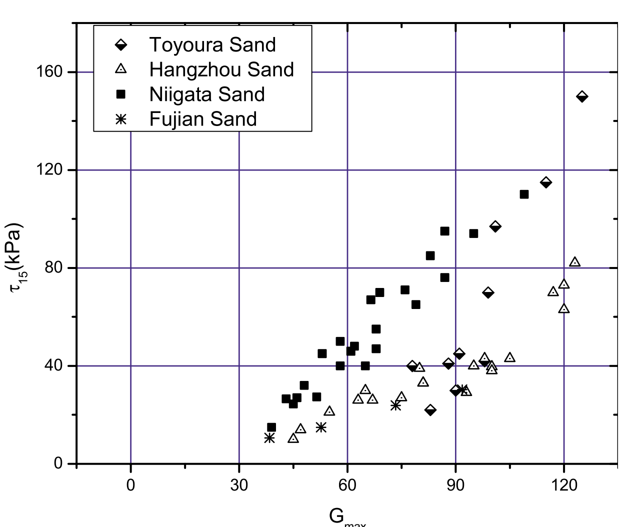

Fig. 6. Relationship between G_{max} and τ_{15} for different sands.

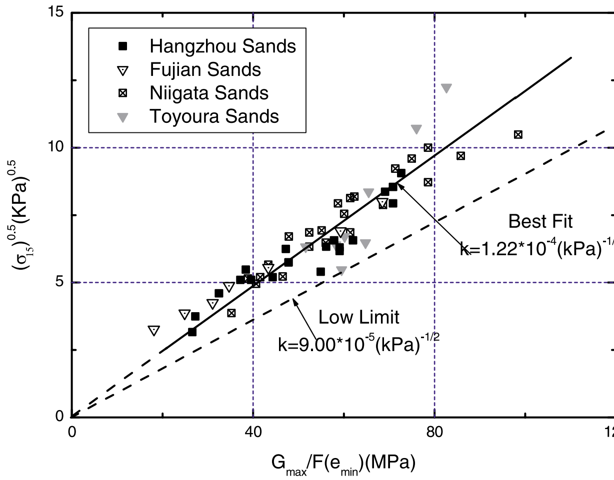

Fig. 7. Relationship between $G_{max}/F(e_{min})$ and $(\tau_{15})^{1/2}$ for different sands.

4. Evaluation procedure

If the slope of the line in Fig. 7 is defined as K, the liquefaction resistance (τ_{15}) can be defined by:

$$\tau_{15} = K^2 G_{max}^2 / F^2(\mathrm{e}_{min}) \tag{5}$$

For a given seismic shear stress and cyclic number, there exists a corresponding critical G_{max} called $(G_{max})_{liq}$ in this paper. If the G_{max} of a soil in situ is greater than $(G_{max})_{liq}$, its liquefaction resistance will be greater than that cyclic stress, and vice versa. So after τ_{15} in Eq. (5) is substituted by $0.65 a_{max} z r_d \bar{\rho}$ [9] and the multi-directional effects is taken into consideration, the corresponding liquefaction threshold value of shear wave velocity V_{sliq} can be defined as follows

$$V_{sliq} = \sqrt{\frac{(G_{max})_{liq}}{\rho}} = \left(\frac{0.65 a_{max} z r_d \bar{\rho} F^2(\mathrm{e}_{min})}{r_c K^2 \rho^2}\right)^{1/4} \tag{6}$$

where

- a_{max} the peak horizontal ground surface acceleration,
- z the depth of the soil in question,
- $\bar{\rho}$ the average density of the soil above the depth in question,
- r_c a constant to account for the effects of multi-directional shaking with a value between 0.9 and 1.0,
- ρ density of the soil in question.
- r_d a shear stress reduction coefficient to adjust for flexibility of the soil profile, average r_d values can be estimated using the following functions [10]:

$$r_d = 1.0 - 0.00765z \quad \text{for } z \leq 9.15 \text{ m} \tag{7a}$$

$$r_d = 1.174 - 0.0267z \quad \text{for } 9.15 \text{ m} < z \leq 23 \text{ m} \tag{7b}$$

$$r_d = 0.744 - 0.008z \quad \text{for } 23 \text{ m} < z \leq 30 \text{ m} \tag{7c}$$

V_{liq} obtained from Eq. (6) can be utilized to estimate the liquefaction susceptibility of a soil or sand during earthquakes. From Fig. 7, the value of 'best fit' K for τ_{15} is 1.22×10^{-4} (kPa)$^{-1/2}$ and low limit value of K is 0.90×10^{-4} (kPa)$^{-1/2}$.

According to Eq. (5), the resistance of the soil to liquefaction CRR, expressed as a cyclic resistance ratio can be defined as follows:

$$\mathrm{CRR} = \frac{K^2 G_{\max}^2}{F^2(\mathrm{e}_{\min})\sigma_0'} \tag{8}$$

Traditionally the magnitude scaling factor is applied to the cyclic resistance ratio called *CRR,* and equals 1.0 for earthquakes with a magnitude 7.5. For magnitudes other than 7.5, the 1996 NCEER workshop (Youd et al., 1997) recommended a range of factors that can be represented by:

$$\mathrm{MSF} = \left(\frac{M_\mathrm{w}}{7.5}\right)^n \tag{9}$$

where M_w, moment magnitude; and n, exponent. The lower bound for the range of MSFs recommended by the 1996 NCEER workshop if defined by $n=-2.56$. The upper bound of the recommended range is defined with $n=-3.3$ (Andrus and Stokoe, 1997) for earthquakes with magnitudes ≤ 7.5.

A typical correlation between the number of cycles and the earthquake magnitude is given by Seed et al. (1985) as shown in Table 2. From this correlation, the best fit and low limit K-value for different number of cycles other than 15 can be calculated as a reference listed in Table 2.

According to Tokimatsu and Uchida [3], if the minimum void ratio needed in Eq. (6) is unknown, a relationship between minimum void ratio and fines content presented by Sakai and Yasuda [11] can be used to evaluate it as the first approximation. On the average the minimum void ratio is 0.65 for sands with fines content less than 20%, 0.75 for silty sands, and 0.95 for sandy silt.

So the procedure for evaluating liquefaction resistance through V_s measurements can be summarized in the following steps:

(1) From subsurface data, develop detailed profiles of V_s, soil type, soil density, and if possible, $e_{\min}$.
(2) Determine the design earthquake magnitude and due value of K (low limit value is recommended in this paper) as well as expected $a_{\max}$.
(3) Calculate V_{sliq} according to Eq. (6) and compare it with V_s for each measurement depth. Liquefaction is predicted to occur when $V_\mathrm{s}<V_{\mathrm{sliq}}$, and not to occur when $V_\mathrm{s}>V_{\mathrm{sliq}}$.

5. Comparison of liquefaction resistance evaluations with other methods and field performance

5.1. Comparison with the procedure proposed by Andrus and Stokoe (1997)

The procedure proposed by Andrus and Stokoe [1] is based on field performance data from 26 earthquakes and in situ V_s measurements from >70 sites in soils ranging from fine sand to sandy gravel with cobbles. It follows the general format of the Seed–Idriss simplified procedure and the liquefaction resistance curves correctly predicted moderate to high liquefaction potential for $>95\%$ of the liquefaction case histories.

Three parameters are required in the evaluation procedure: (1) the level of cyclic loading on the soil caused earthquake CSR, expressed as a cyclic stress ratio; (2) stiffness of soil, expressed as an overburden stress-corrected shear wave velocity V_{s1}; and (3) resistance of the soil to liquefaction CRR, expressed as a cyclic resistance ratio.

CSR equals CRR at the point separating liquefaction and non-liquefaction. Andrus and Stokoe (1997) proposed the $\mathrm{CRR}-V_{\mathrm{s1}}$ relationship based on the concept of constant average cyclic shear strain suggested by R. Dobry, and they modified this relation in 2000 as follows

$$\mathrm{CRR} = \left\{ a\left(\frac{V_{\mathrm{s1}}}{100}\right)^2 + b\left(\frac{1}{V_{\mathrm{s1}}^* - V_{\mathrm{s1}}} - \frac{1}{V_{s1}^*}\right)\right\}\mathrm{MSF} \tag{10}$$

where V_{s1}^*, limiting upper value of V_{s1} for cyclic liquefaction occurrence; a and b, curve fitting parameters; and MSF, Magnitude scaling factor to account for the effect of earthquake magnitude.

By combing (8) and $G_{\max}=\rho V_\mathrm{s}^2$, the cyclic resistance ratio CRR can be obtained as follows:

$$\mathrm{CRR} = \frac{K^2\rho^2}{F^2(\mathrm{e}_{\min})\sigma_0'} V_\mathrm{s}^4 \tag{11}$$

Assuming 15 loading times, parameters are adopted as follows: $K=1.22\times10^{-4}$(kPa)$^{-1/2}$ (best fit), $K=9.00\times10^{-5}$(kPa)$^{-1/2}$ (low limit), $\rho=1.85$ g/cm^3, $e_{\min}=0.65$ [11], $\sigma_0'=100$ kPa. The CRR obtained from Eq. (11) and that

Table 2
The value of K for different cycles

Earthquake magnitude	5–1/4	6	6–3/4	7–1/2	8–1/2
Numbers of representative cycles	2–3	5	10	15	26
$n=-2.56$, 10^{-4}(kPa)$^{-1/2}$ (best fit)	1.92	1.62	1.40	1.22	1.03
$n=-3.3$, 10^{-4}(kPa)$^{-1/2}$(best fit)	2.20	1.76	1.45	1.22	0.99
$n=-2.56$, 10^{-4}(kPa)$^{-1/2}$ (low limit)	1.42	1.20	1.03	0.90	0.77
$n=-3.3$, 10^{-4}(kPa)$^{-1/2}$(low limit)	1.62	1.30	1.07	0.90	0.73

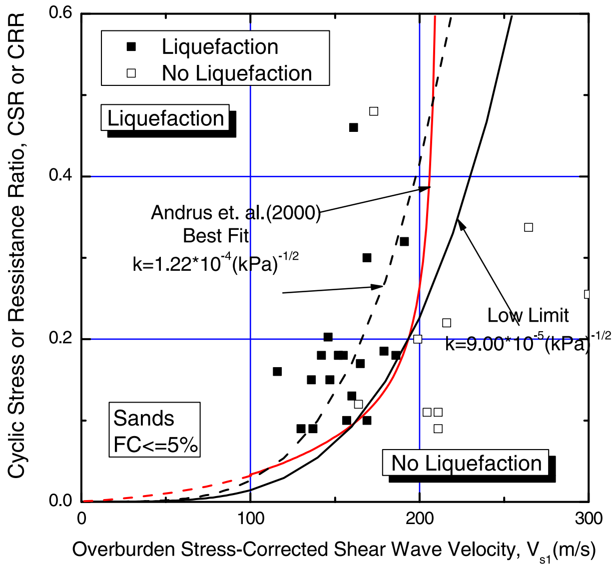

Fig. 8. Correlation curves between CRR and V_{sl} for sands with lower fines content.

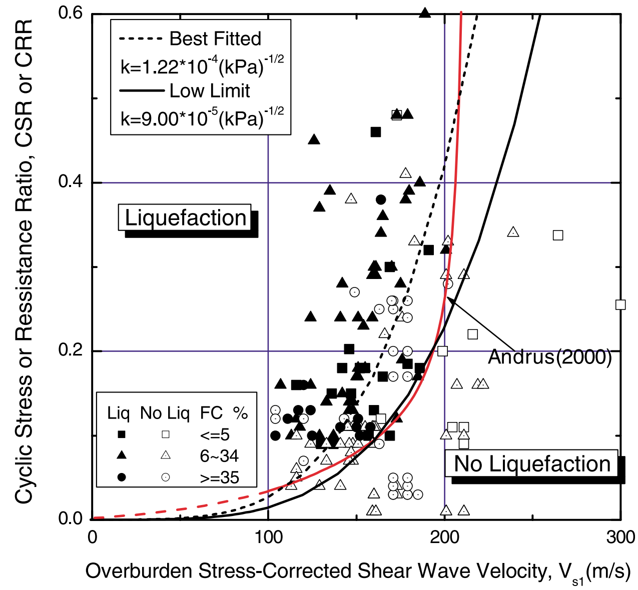

Fig. 9. Correlation curves between CRR and V_{sl} for sands with different fines content.

presented by Andrus et al. [1] as well as in situ measurement data are plotted in Fig. 8.

It is seen that the correlation curve presented in this paper with low limit value of K agree well with the curve proposed by Andrus et al. [1] when the corrected shear wave velocity is between 120 and 200 m/s. But the curve of Andrus becomes more close to the curve with best fit value of K in this paper with higher corrected shear wave velocity. This comparison result demonstrates that the correlation presented in this paper is more conservative than Andrus et al. [1] with higher terms of shear wave velocity. Generally speaking, the correlation described by means of Eq. (11) with low limit value of K can separate the in situ measurements data successfully. However, it should be pointed out as previously that the liquefaction criterion adopted for lab results (strain criterion) is not consistent with field evaluation completely, since usually the field liquefaction is defined based on pore pressure.

Unexpectedly, the curves proposed in this paper also obtain satisfactory results when applied to sand of higher terms of fines content (Fig. 9) assuming $e_{min}=0.65$.This result implies that the correlation represented by Eq. (10) may overestimate the low limit CRR of sand with high fines content. This result may induced by the fact that the effectiveness of normalization with e_{min} is validated from laboratory tests on only four kinds of sands, it need further validation or modification especially when applied to 'low limit' CRR. From the view of safety, 0.65 is recommended for e_{min} in this procedure when it is more than 0.65.

5.2. Comparison with other CRR–V_{sl} curves

Andrus and Stokoe [1] compared their CRR–V_{sl} curve with other CRR–V_{sl} curves proposed by Andrus and Stokoe (1997), [12], Kayen et al. (1992), [7], and Tokimatsu and Uchida [3] (best fit and low bound), respectively. Fig. 10 compares the CRR–V_{sl} curve proposed in this paper and those curves after Andrus and Stokoe [1]. It is shown that the low limit boundaries in this paper and Tokimatsu and Uchida [3] are close to the curve proposed by Andrus and Stokoe [1] whose procedure is recommended by the 1996 NCEER workshop in the range of V_{sl} of 100–200 m/s, with which engineers may most concerned. The best-fit curve in this paper, is drawn close to the best fit curve proposed by Tokimatsu and Uchida [3] as expected. Generally speaking, the curves obtained in this paper are located within the

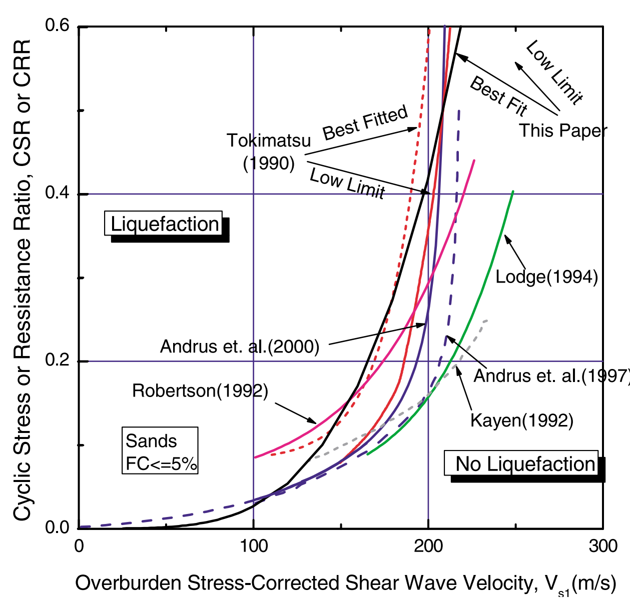

Fig. 10. Comparison of boundaries from different research results.

boundaries from other research results and agree well with data collected from sites.

Two zones are still debatable from the comparison result from Fig. 7: V_{sl} is less than 100 m/s or greater than 200 m/s especially 210 m/s. This is mainly due to the shortage of data of occurrence of liquefaction in these zones. For example, it is shown that the CRR–V_{sl} curves obtained in this paper are obviously conservative than other curves when V_{sl} is 100 m/s or less. The curves from Andrus et al. (1997, [3]) is based on the concept of average cyclic shear strain which implied the CRR is linear with V_{sl}^2. When it is extended to the high value of shear wave velocity, under-estimated CRR is obtained. For this reason, the second term in Eq. (10) is added as a moderation. According to Eq. (11), CRR is linear with V_S^4 approximately and the under-estimated CRR can be avoided reasonably. However, by comparison both with the curves presented by Tokimatsu and Uchida [3] and Andrus and Stokoe [1], the CRR computed by this procedure with low limit value of K is still under-estimated to some extent. This result may induced by dilation [1]. Further investigation by means of in situ measurements and laboratory tests should be applied to validate or moderate the relation in this paper.

5.3. Case study

To validate the evaluation procedure in this paper further, the case study discussed by Andrus [1] is utilized. The site is Treasure Island Fire Station which was shaken by the 1989 Loma Prieta, California, earthquake ($M_w = 7$). The values of shear wave velocity measured by cross-hole testing and the CSR are shown in Fig. 11(a) and (b), respectively. These values were calculated assuming soil densities of 1.76 Mg/m^3 above the water table and 1.92 Mg/m^3 below the water table. A geometric mean value 0.13 g is assumed for a_{max} and the average values originally proposed by Seed and Idriss (1971) are assumed for r_d. Profiles of soil type and fines content were based on information provided by de Alba et al. (1994) and de Alba and Faris (1996). Values of CRR calculated by Andrus [1] and the procedure proposed in this paper are also shown in Fig. 11(b). Value for MSF is assumed to be 1.19, the lower bound value recommended by the 1996 NCEER workshop (Youd et al., 1997), and due low bound K value is 0.983.

Two series of e_{min} are assumed for the calculation of CRR from Eq. (11). One is based on the suggestion proposed by Tokimatsu and Uchida [3], 0.75 for silty sands and 0.95 for sandy silt (Series 2). Value assumed for all the soil in the other series calculation is 0.65 (Series 1), since 0.65 is assumed when applied to the comparison with the curves presented by Andrus [1] and obtain satisfactory result. It is shown as expected that the calculation results of Series 1 agree well with those presented by Andrus [1] since the correlation between the CRR and critical V_{sl} or V_{sliq} and the correlation between V_{sl} or V_{sliq} and depth are close to each other. As discussed by Andrus [1], between the depths of 7 and 9 m, the soil exhibits plastic characteristics and may be non-liquefiable by the Chinese criteria. So the layer most likely to liquefy, or the critical, lies between the depths of 4 and 7 m. The estimation of liquefiable zone according Series 1 agree with this conclusion since the soil below 12 m also exhibits plastic characteristics. The non-liquefiable zone due to plastic characteristics can be distinguished in Series 2. Besides, the CRR of Series 2 are much greater than other two and only one point is predicted to be susceptible to liquefaction. During the 1989 Loma Prieta earthquake, there is a sudden drop in the recorded

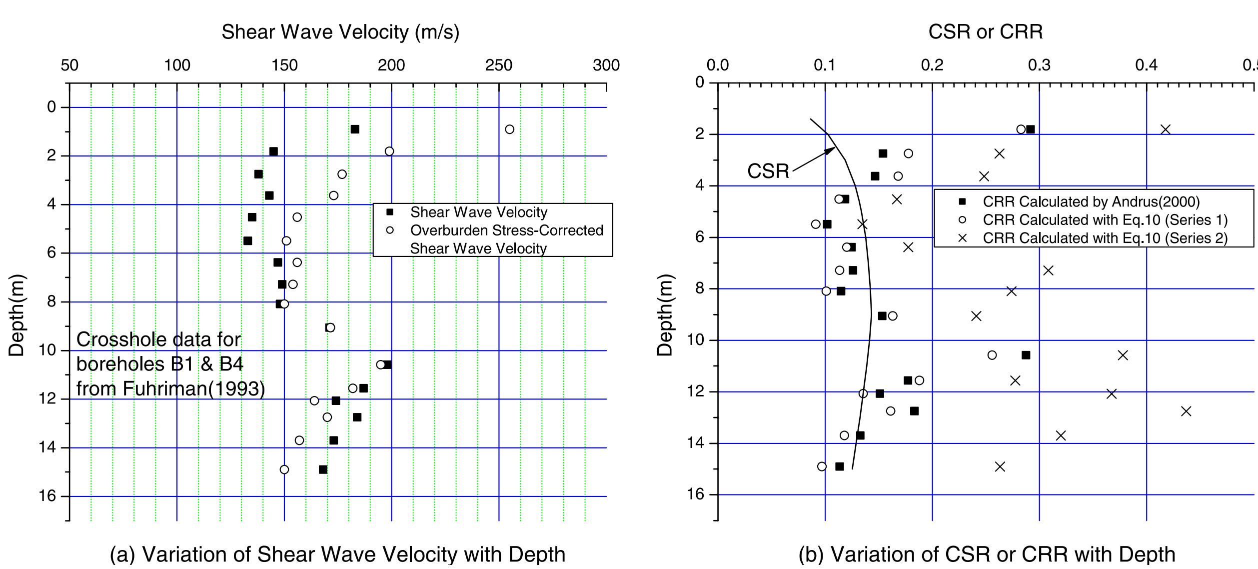

Fig. 11. Comparison of the procedures presented in this paper and Andrus [1] when applied to TI fire station.

acceleration at about 15 s and small motion afterwards (Idriss, 1990). De Alba et al. (1994) attribute this behavior to liquefaction of an underlying sand. However, no boils or ground cracks occurred at the site. So it is hard to determine whether Series 2 or Series 1 as well as those presented by Andrus [1] are more close to the facts. Generally speaking, the influence of soil diversity (e.g. plastic characteristics) can be considered in Series 2 to some extent, but it may overestimate this influence and more investigation (laboratory and field performance) is needed to validate or modify it. Again, 0.65 is recommended for $e_{\min}$ of silty sand in this procedure or the $e_{\min}$ of the sand is more than 0.65.

6. Further discussion

The method proposed by Tokimatsu and Uchida' [3] is simplified mainly in that the equation presented in this paper does not have to consider the influence of confining pressure on critical shear wave velocity. The effect of effective stress is embodied in the in situ shear wave velocity. For example, supposing points A and B are at the same depth in Fig. 12 and the parameters of Eq. (6) for A and B are the same, they have the same V_{sliq} according to Eq. (6). If the perennial water level of point A is lower than that of point B, A's effective stress should be greater than B's. If other conditions are all the same, A's in situ shear wave velocity should be greater than B's, so B is more susceptible to liquefaction.

Both liquefaction potential and shear wave velocity are influenced by other factors not embodied in Eq. (11), such as stability of fabric, K_0, prior strain history and over-consolidation. Their effects can be explained in the same way.

Because of the power correlation of 1/4, the error of V_{sliq} is only about 10% when the error of $0.65a_{\max}d_s r_d\bar{\rho}F^2(e_{\min})/r_c K^2\rho^2$ amounts to 40% (most of it come from $F(e_{\min})$ and K). Since the results of shear wave test in situ are also very stable, the shear wave testing has higher stability. Considering Eq. (6) is easy to calculate and every parameter has an explicit meaning and is not difficult to obtain, more and more engineers is believed to extend its applications.

In addition, when the n in Eq. (4) changes from 2/5 to 2/3, the power of 1/4 in Eq. (11) will be changed from 1/5 to 1/3 with the overall form of Eq. (11) unchanged as long as the good correlation still exists. Of course, it is suitable to define n as 0.5, or say, the exponent equal to 1/4 in Eq. (11) for most cases.

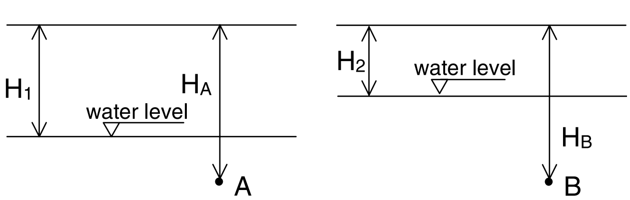

Fig. 12. Comparison about V_{scr} based on Eq. (10) and the V_s in situ between two points with different water level at the same depth.

7. Conclusions

In this paper, a simplified procedure is proposed based on the combination of in situ measurements of shear wave velocity and laboratory tests for evaluating liquefaction resistance though shear wave velocity. The CRR–V_{sl} curves converted from this procedure with low limit K-value agree well with the curve presented by Andrus and Stokoe [1] in the range of V_{sl} 100–200 m/s. Further field performance and laboratory tests are required to validate or improve this method especially when applying to the site when V_{sl} is less than 100 m/s or greater than 200 m/s and sands with higher fines content.

One of the major simplifications of this procedure is that it is shear stress other than shear stress ration is adopted in the evaluation of liquefaction resistance. This simplification is based on the test results which imply a reasonable good relation would exist between liquefaction characteristics and the elastic shear modulus for given soil irrespective confining stress. Also further laboratory tests are required to validate or improve this assumption especially when applying to the soil with especially low or high shear modulus.

Appendix

The following symbols and notation are used in this report:

A	parameter that depends on the soil structure
$a_{\max}$	peak horizontal ground surface acceleration;
D_{10}	diameter of grain of which 10% by weight smaller
e	void ratio
$e_{\max}$	maximum void ratio
$e_{\min}$	minimum void ratio
$F_c(\%)$	fines content (particle smaller than 75 μm
$F(e)$	function of void ratio
$F(e_{\min})$	function of minimum void ratio
g	acceleration of gravity
$(G/G_{\max})_{\gamma_t}$	dynamic shear modulus ratio when the shear strain is γ_t.
$G_{\max}$	small-strain shear modulus
$(G_{\max})_{\text{liq}}$	liquefaction threshold value of $G_{\max}$ for a given

seismic cyclic stress	
G_s	specific gravity of solids
G_0	G_{max} under a given situation (e.g. the relative density is 60% and the confining pressure is 100 kPa for PA samples)
K	slope of $(\tau_d)^{1/2} - G_{max}/F(e_{min})$ curve
k_0	coefficient of lateral earth pressure at rest
n	a constant exponent
OC sample	sample experienced overconsolidation history
P_a	a reference stress, 100 kPa or approximately atmospheric pressure
PA sample	sample obtained by pluviation through air
r_c	multi-directional shaking correction factor
r_d	stress reduction factor with depth
SH sample	sample subjected to small seismic strain history
U_c	coefficient of uniformity
V_s	small-strain shear wave velocity
V_{scr}	limiting upper value of V_s for liquefaction occurrence
V_{sliq}	liquefaction threshold value of shear wave velocity
V_{s1}	overburden stress-corrected V_s
z	the depth of the soil;
γ_t	threshold shear strain
ρ	mass density of soil
$\bar{\rho}$	average density of the soil above the depth in question,
$\sigma_d/2$	liquefaction resistance
σ'_m	mean effective confining stress
σ'_v	the vertical effective confining stress
τ_d	$\sigma_d/2$, liquefaction resistance
τ_0	τ_d under a given situation (e.g. the relative density is 60% and the confining pressure is 100 kPa for PA samples)
τ_{15}	liquefaction resistance causing a double amplitude axial strain of 5% in 15 cycles

References

[1] Andrus RD, Stokoe KH. Liquefaction resistance of soils from shear-wave velocity. J Geotech Geoenviron Eng 2000;126(11):1015–25.

[2] Shi ZJ. A method to evaluate the liquefaction potential of horizontal layered sands with shear wave velocities. Hydrogeol Eng Geol 1986;(4):74–80 (in Chinese).

[3] Tokimatsu K, Uchida A. Correlation between liquefaction resistance and shear wave velocity. Soils Found 1990;30(2):33–42.

[4] De Alba P, Baldwon K, Janoo V, Roe G, Celikkol B. Elastic-wave velocities and liquefaction potential. Geotech Test J 1984;7(2):77–88.

[5] KH Stokoe, JM Rosset, JG Bierschwale, Aouad M. Liquefaction potential of sands from shear wave velocity. Proceedings of the ninth world conference on earthquake engineering, Tokyo, Japan, vol. 3; 1988, p. 213–18.

[6] Seed HB, Idriss IM, Arango I. Evaluation of liquefaction potential using field performance data. J Geotech Eng, ASCE 1983;109(3):458–82.

[7] Lodge AL. Shear wave velocity measurements for subsurface characterization. PhD Dissertation. Berkeley, CA: University of California; 1994.

[8] Tokimatsu K, Yamazaki T, Yoshimi Y. Soil liquefaction evaluation by elastic shear moduli. Soils Found 1986;26(1):25–35.

[9] Seed HB. Soil liquefaction and cyclic mobility evaluation for level ground during earthquakes. J Geotech Eng Div, ASCE 1979;105(GT2):201–55.

[10] Liao SSC, Whitman RV. Overburden correction factors for SPT in sands. J Geotech Eng Div, ASCE 1986;112(3):373–7.

[11] Sakai Y, Yasuda S. Liquefaction characteristics of undisturbed sandy soils. Proceedings of the 12th Annual Meeting JSSMFE; 1977, p. 389–92 [in Japanese].

[12] Robertson PK, Woeller DJ, Finn WDL. Seismic cone penetration test for evaluating liquefaction potential under cyclic loading. Can Geotech J 1992;29:686–95.

[13] Dobry R, Powell DJ, Yokel FY, Ladd RS. Liquefaction potential of saturated sand—the stiffness method. Proceedings of the seventh world conference on earthquake engineering, Istanbul, Turkey, vol. 3; September, 1986, p. 25–32.

[14] Huang B, Yin JH, Chen YM, Wu SM. Measurements of Elastic Shear Modulus Gm Using Piezoceramic Bender Elements. Chinese J Vib Eng 2001;14(2):155–60.

[15] Zhou YG, Chen YM. Influence of seismic cyclic loading history on small strain shear modulus of saturated sand. Soil Dyn Earthquake Eng 2005;25(5):341–53.